Floor fractured craters on the Moon: An evidence of past intrusive magmatic activity ?

Clément Thorey[1] and Chloé Michaut[1], [1]Institut de Physique du Globe, Université Paris-Diderot, Sorbonne Paris cité, UMR 7154, Paris, France (thorey@ipgp.fr)

Introduction

Intrusive magmatism on the Moon should be an important aspect of lunar evolution given the low-density of its anorthositic crust and the high density of the iron-rich mare basaltic lavas. We look for evidence of magmatic intrusions to help quantify the ratio of intrusive to extrusive magmatism, which is an elusive quantity for all planets, including Earth. *Schultz* [1] proposed that magmatic intrusions may be the main mechanism leading to the secondary floor modification observed at Floor-Fractured Craters (FFC's) which are a class of craters modified by post impact mechanisms. FFC's are defined by shallow floors with a plate-like or convex appearance, wide floor moats and radial, concentric and polygonal floor-fractures, suggesting an endogenous process of modification. Viscous relaxation has also been proposed to explain the observed deformation [*Dombard et al.* [2]]. Here, we test the case of magmatic intrusions. We develop a model for the dynamics of magma spreading below an elastic crust with a crater-like topography and above a rigid horizontal surface. We show that this model can explain most of the morphological features observed at FFC's.
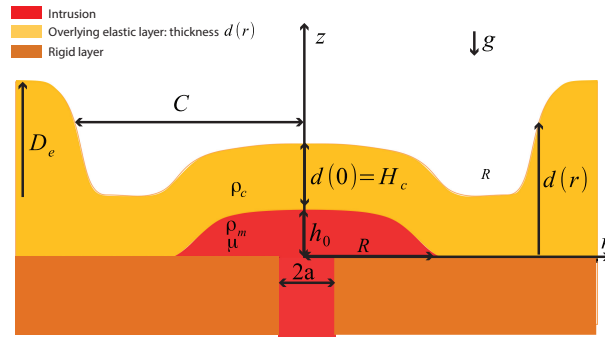
Axisymmetric model

Figure 1: Sketch of the intrusion spreading below an impact crater topography. De (resp. C) represents the depth (resp. radius) of the impact crater. The intrusion spreads above a rigid homogeneous and horizontal bed rock at depth $d(r)$ below the crater floor. At the center, the intrusion depth is noted H_c.

In this axisymmetric model, we consider the spreading of an isoviscous magma: at the center of the impact crater, the intrusion occurs at depth H_c below the crater floor (Figure 1). The magma spreads along a horizontal bedding plane and we neglect fracturing at the tip. The magma injection rate, noted Q_0, is considered constant through a dyke of radius a. The layer above the intrusion deforms elastically; it is characterized by its flexural parameter Λ that represents the minimum wavelength over which the layer can support elastic stresses [*Michaut* [3]]:

$$\Lambda = \left(\frac{EH_c^3}{12(1-\nu^2)\rho_m g} \right)^{\frac{1}{4}} \tag{1}$$

where E, the Young's modulus, ν, the Poisson's ratio, g, the gravity and ρ_m, the magma density. For given elastic properties for the upper layer, the flexural wavelength of the elastic layer increases with the intrusion depth.

Dimensionless numbers

An equation for the evolution of the flow thickness as a function of time and radial coordinates can be found by writing the conservation of momentum and the mass conservation integrated over the flow thickness. This equation is composed of three different terms: a gravity current term accounting for the spreading of the flow under its own weight, an elastic term representing the squeezing of the flow by the overlying layer and a last term accounting for the increase in the lithostatic pressure at the crater rim. The nondimensionalization of this equation leads to the identification of three main dimensionless numbers governing the flow dynamics and hence, the deformation of the crater floor:

$$\Xi \quad = \quad \left(\frac{\rho_c g D_e}{\rho_m g H} \right) \tag{2}$$

$$\Theta \quad = \quad \left(\frac{\Lambda}{C} \right)^4 \tag{3}$$

$$\Psi \quad = \quad \frac{D_e}{H_c} \tag{4}$$

where $H = \left(\frac{12\mu Q_0}{\rho_m g \pi} \right)^{\frac{1}{4}}$ is a characteristic scale for the thickness of a gravity current and μ, the magma viscosity.

Ξ represents the effect of the lithostatic pressure increase at the rim, Θ characterizes the wavelength of the elastic deformation relatively to the crater radius and Ψ characterizes the elastic thickening below the crater rim.

2

Results and predicted deformations

Numerical results show that the lithostatic pressure increase at the crater rim Ξ prevents the intrusion from spreading horizontally. Therefore, once the intrusion radius reaches the crater radius, the intrusion thickens which causes an uplift of the crater floor (Figure 2). Furthermore, the deformation of the overlying layer exerts a strong control on the intrusion shape, and hence, on the nature of the crater floor uplift. The intrusion shape shows a bell-shaped geometry for crater radius smaller than 4Λ, or a flat top with bell-shaped edges for crater radius larger than 4Λ. Then, for deep intrusions or small craters, i.e. large values of the dimensionless flexural parameter such that $\Theta > 10^{-3}$, the crater floor undergoes a convex uplift (Figure 2: right). On the contrary, for shallow intrusions or large craters, i.e. small values of the dimensionless flexural parameter such that $\Theta < 10^{-3}$, we observe a piston-like uplift of the central part of the crater floor with the formation of moats adjacent to the rim whose size is about 4Λ (Figure 2: left). Finally, an increase in the thickening of the elastic layer Ψ leads to an increase in the depth of the moats.

Depth of intrusion

Our model can be used to predict the intrusion depth. The newly available Lunar Reconnaissance Orbiter (LRO) Lunar Orbiter Laser Altimeter (LOLA) image data provide new constraints for the shape and topography of these FFC's [*Jozwiak et al.* [4]]. By comparing the crater floor topography obtained with these data with the floor appearance obtained in our simulation, we can estimate a corresponding range of values for the dimensionless number Θ. Then, given the crater radius, we can estimate a range of values for Λ and hence constrain the intrusion depth. For instance, Vitello, a FFC located along the southern edge of the small Mare Humorum, shows a large convex floor characterized by a value of the number Θ between 10^{-3} and 10^{-2} (Figure 2: right). We then estimate the intrusion depth to be between 3 and 5 km. For Warner, a FFC located in the southern part of the Mare Smythii, the deformation shows a plate-like central floor with wide moats characterized by a smaller value of the number Θ of about 10^{-4} (Figure 2: left). In this case, the intrusion depth should range between $0.5 - 1.2$ km.

Conclusion

On the contrary to viscous relaxation models, our model is thus able to reproduce most of the features of FFC's, including small-scale features. Spreading of a magmatic intrusion at depth can thus be considered as the main endogenous mechanism at the origin of the deformations
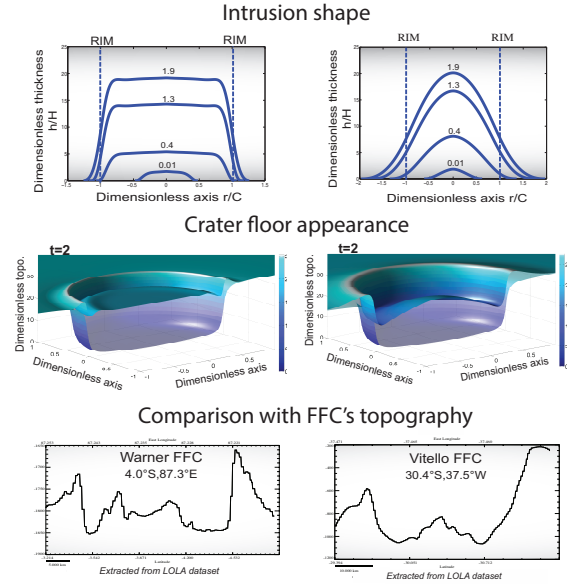

Figure 2: **Left**: $\Theta = 10^{-5}, \Psi = 0.3$. **Right**: $\Theta = 10^{-2}, \Psi = 0.3$. **Top**: Profile of the intrusion at different times t/τ with $\tau = \frac{\pi C^2 H}{Q_0}$ indicated on the plot. Variables are dimensionless. **Middle**: Dimensionless topography of the crater, final deformation is superimposed to the initial complex crater (transparent). **Bottom** Topography profiles extracted from the LOLA dataset showing the two different types of floor appearances observed at FFC: flat and shallow with moat adjacent to the rim (Warner, left) and convex (Vitello, right).

observed at FFC's. Given the large numbers of FFC's observed at the lunar surface, magmatic intrusion seems to be an important process to take into account in lunar geological evolution models as well as to explain geological and geophysical data from the Moon.

References

[1] Schultz, P. H., *The Moon*, 15, 241-273, 1976

[2] Dombard, A. J. and Gillis, J. J., *J. Geophys. Res.*, 106, 27901-27909, *doi:10.1029/2000JE001388*, 2001

[3] Michaut C., *J. Geophys. Res.*, 116, B5, *doi:10.1029/2010JB008108*, 2010

[4] Jozwiak, L. M., Head J. W., Zuber M. T., Smith E. D., *J. Geophys. Res.*, 117, *doi:10.1029/2012JE004134*, 2012